Supramolecular self-associating amphiphiles inhibit biofilm formation by the critical pathogens, *Pseudomonas aeruginosa* and *Candida albicans*

Hendrik J. F. Steyn,[a] Lisa J. White,[b] Kira L. F. Hilton,[b] Jennifer R. Hiscock,[b]* Carolina H. Pohl[a]*

Corresponding Authors

Carolina H. Pohl – Department of Microbiology and Biochemistry, Faculty of Natural and Agricultural Sciences, University of the Free State, Free State, South Africa, 9301; E-mail: PohlCH@ufs.ac.za

Jennifer R. Hiscock – School of Chemistry and Forensics, University of Kent, Canterbury, United Kingdom, CT2 7NH; E-mail: J.R.Hiscock@kent.ac.uk

Contents

Experimental

General Remarks. A positive pressure of nitrogen and oven dried glassware were used for all reactions. All solvents and starting materials were purchased from known chemical suppliers or available stores and used without any further purification unless specifically stipulated. The NMR spectra were obtained using a Burker AV2 400 MHz or AVNEO 400 MHz spectrometer. The data was processed using Bruker Topspin software. NMR Chemical shift values are reported in parts per million (ppm) and calibrated to the centre of the residual solvent peak set (s = singlet, br = broad, d = doublet, t = triplet, q = quartet, m = multiplet).

Anti-Biofilm Activity of Currently Available and Marketed Antimicrobials

Metabolic Activity Assay for Inhibition of Biofilm Formation. *P. aeruginosa* and *C. albicans* mono- and polymicrobial biofilms were cultivated for 48 hours at 37 °C as described previously [7-9] in the presence of selected antimicrobials (0.25 – 512 µg.mL^{-1}). After incubation, an indirect and semi-quantitative measure of biofilm formation was performed, using a 2,3-bis(2-methoxy-4-nitro-5-sulfo-phenyl-)-2H-tetrazolium-5-carboxanilide (XTT) colourimetric reduction assay as described using 1 g.L^{-1} of filter sterilized (0.22 µm nitrocellulose filter) XTT salt (Sigma-Aldrich, United Kingdom), dissolved in PBS and supplemented with 1 mM menadione in acetone. The supernatant from the 96-well plates was discarded, the wells washed twice with 200 µL PBS before 50 µL of XTT-menadione solution was introduced to each well. The plates were incubated for 3 hours at 37 °C in the dark and the absorbance measured at 492 nm using a microtitre plate reader (EZ Read 800 Research, Biochrom, England). Cell-free solvent controls and negative controls were included and the percentage inhibition, relative to the negative control, was calculated. These experiments were performed in technical triplicates and biological duplicates.

Chemical Structures

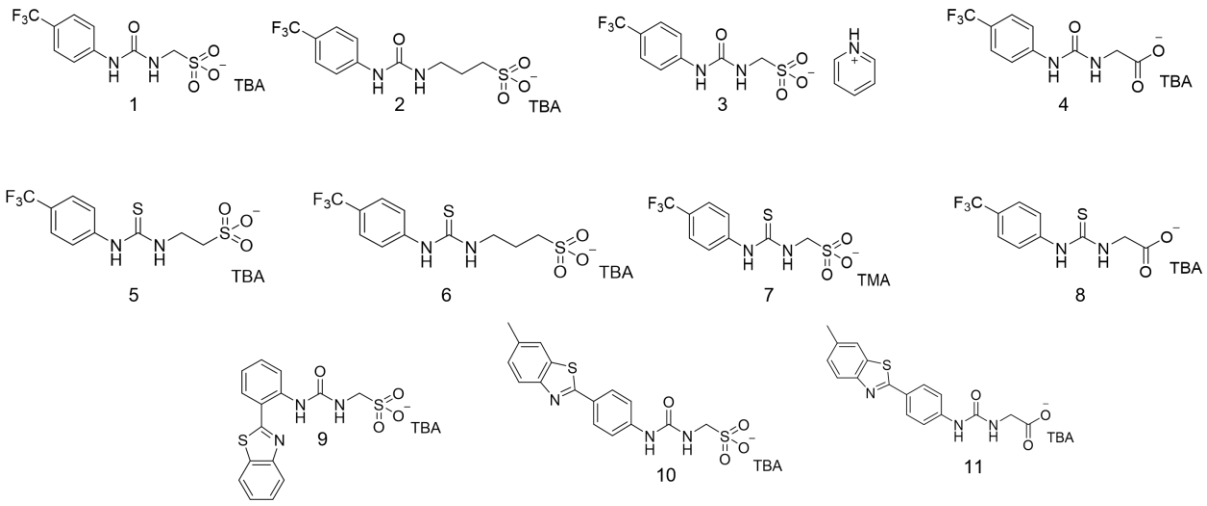

Figure S1. Chemical structures of SSAs **1** - **11**. TBA = tetrabutylammonium. TMA = tetramethylammonium.

Chemical Synthesis

Compound 1: This compound was synthesised in line with our previously published methods. Proton NMR was found to match our previously published values.[1] ^{1}H NMR (400 MHz, 298.15 K, DMSO-d_6): δ: 9.20 (s, 1H), 7.55 (s, 4H), 6.69 (s, 1H), 3.88 (d, *J*

= 5.84 Hz, 2H), 3.18 - 3.14 (m, 8H), 1.58 - 1.52 (m, 8H), 1.33 - 1.28 (m, 8H), 0.93 (t, *J* = 6.95 Hz, 12H).

Compound 2: This compound was synthesised in line with our previously published methods. Proton NMR was found to match our previously published values.[2] ^{1}H NMR (400 MHz, 298.15 K, DMSO-d_6): δ: 9.04 (s, 1H), 7.56 (dd, *J* = 30.88, 8.64 Hz, 4H), 6.58 (t, *J* = 6.04 Hz, 1H), 3.17 - 3.14 (m, 10H), 2.49 - 2.47 (m, 2H), 1.76 - 1.72 (m, 2H), 1.60-1.52 (m, 8H), 1.35 - 1.28 (m, 8H), 0.92 (t, *J* = 7.28 Hz, 12H).

Compound 3: This compound was synthesised in line with our previously published methods. Proton NMR was found to match our previously published values.[3] ^{1}H NMR (400 MHz, 298.15 K, DMSO-d_6): δ: 9.20 (s, 1H), 8.90 (d, *J* = 5.08 Hz, 2H), 8.57 (t, *J* = 7.88 Hz, 1H), 8.04 (t, *J* = 6.52 Hz, 2H), 7.50 (q, *J* = 8.84 Hz 4H), 6.90 (s, 1H), 3.92 (d, *J* = 5.48 Hz, 2H).

Compound 4: This compound was synthesised in line with our previously published methods. Proton NMR was found to match our previously published values.[4] ^{1}H NMR (400 MHz, 298.15 K, DMSO-d_6): δ: 10.41 (s, 1H), 7.70 (d, *J* = 8.56 Hz, 2H), 7.49 (d, *J* = 8.68 Hz, 2H), 6.86 (s, 1H), 3.35 (s, 2H), 3.17 - 3.13 (m, 8H), 1.60 - 1.52 (m, 8H), 1.34 - 1.25 (m, 8H), 0.92 (t, *J* = 6.80 Hz, 12H).

Compound 5: This compound was synthesised in line with our previously published methods. Proton NMR was found to match our previously published values.[4] ^{1}H NMR (400 MHz, 298.15 K, DMSO-d_6): δ: 10.20 (s, 1H), 8.21 (s, 1H), 7.74 (d, *J* = 8.44 Hz, 2H), 7.61 (d, *J* = 7.96 Hz, 2H), 3.56 (s, 2H), 3.18 – 3.14 (m, 8H), 2.68 (t, *J* = 5.44 Hz, 2H), 1.60 - 1.52 (m, 8H), 1.35 - 1.26 (m, 8H), 0.92 (t, *J* = 7.24 Hz, 12H).

Compound 6: This compound was synthesised in line with our previously published methods. Proton NMR was found to match our previously published values.[4] ^{1}H NMR (400 MHz, 333.15 K, DMSO-d_6): δ: 9.89 (s, 1H), 8.20 (s, 1H), 7.77 (d, *J* = 8.10 Hz, 2H), 7.62 (d, *J* = 8.66 Hz, 2H), 3.56 (d, *J* = 5.29 Hz, 2H), 3.17 - 3.14 (m, 8H), 2.50 – 2.46 (m, 2H), 1.89 – 1.81 (m, 2H), 1.60 - 1.53 (m, 8H), 1.35 - 1.26 (m, 8H), 0.93 (t, *J* = 7.32 Hz, 12H).

Compound 7: This compound was synthesised in line with our previously published methods. Proton NMR was found to match our previously published values.[4] ^{1}H NMR

(400 MHz, 333.15 K, DMSO-d_6): δ: 10.29 (s, 1H), 8.05 (s, 1H), 7.84 (d, *J* = 8.56 Hz, 2H), 7.61 (d, *J* = 8.08 2H), 4.26 (s, 2H), 3.13 (s, 12H).

Compound 8: This compound was synthesised in line with our previously published methods. Proton NMR was found to match our previously published values.[4] ^{1}H NMR (400 MHz, 298.15 K, DMSO-d_6): δ: 12.32 (s, 1H), 8.77 (s, 1H), 8.36 (d, *J* = 8.28 Hz, 2H), 7.54 (d, *J* = 8.96 Hz, 2H), 3.71 (s, 2H), 3.16 - 3.12 (m, 8H), 1.58 - 1.50 (m, 8H), 1.33 - 1.24 (m, 8H), 0.91 (t, *J* = 6.56 Hz, 12H).

Compound 9: This compound was synthesised in line with our previously published methods. Proton NMR was found to match our previously published values.[5] ^{1}H NMR (400 MHz, 298.15 K, DMSO-d_6): δ: 10.63 (s, 1H) 8.45 (d, *J* = 8.36 Hz, 1H), 8.31 (d, *J* = 8.36 Hz, 1H), 8.14 (d, *J* = 7.88 Hz, 1H), 7.83 (d, *J* = 7.76 Hz, 2H), 7.58 (t, *J* = 8.04 Hz, 1H), 7.47 (tt, *J* = 11.69, 7.49 Hz, 2H), 7.10 (t, *J* = 7.52 Hz, 1H), 3.95 (s, 2H), 3.16 – 3.14 (m, 8H), 1.58 – 1.53 (m, 8H), 1.32 – 1.27 (m, 8H), 0.92 (t, *J* = 7.24 Hz, 12H).

Compound 10: This compound was synthesised in line with our previously published methods. Proton NMR was found to match our previously published values.[5] ^{1}H NMR (400 MHz, 298.15 K, DMSO-d_6): δ: 9.15 (s, 1H), 7.95 – 7.86 (m, 4H), 7.55 (d, *J* = 9.32 Hz, 2H), 7.32 (d, *J* = 8.64 Hz, 2H), 6.56 (s, 1H), 3.88 (d, *J* = 5.76 Hz, 2H), 3.18 – 3.14 (m, 8H), 2.43 (s, 3H), 1.60 – 1.53 (m, 8H), 1.35 – 1.26 (m, 8H), 0.93 (t, *J* = 7.24 Hz, 12H).

Compound 11: This compound was synthesised in line with our previously published methods. Proton NMR was found to match our previously published values.[6] ^{1}H NMR (400 MHz, 298.15 K, DMSO-d_6): δ: 10.00 (s, 1H), 7.87 (t, *J* = 9.08 Hz, 2H), 7.64 (d, *J* = 8.76 Hz, 2H), 7.32, (d, *J* = 1.08 Hz, 1H), 6.63 (s, 1H), 3.31 (s, 2H), 3.17 – 3.13 (m, 8H), 2.44 (s, 3H), 1.60 – 1.52 (m, 8H), 1.33 – 1.27 (m, 8H), 0.92 (t, *J* = 7.24, 12H).

NMR

NMR Characterisation Data

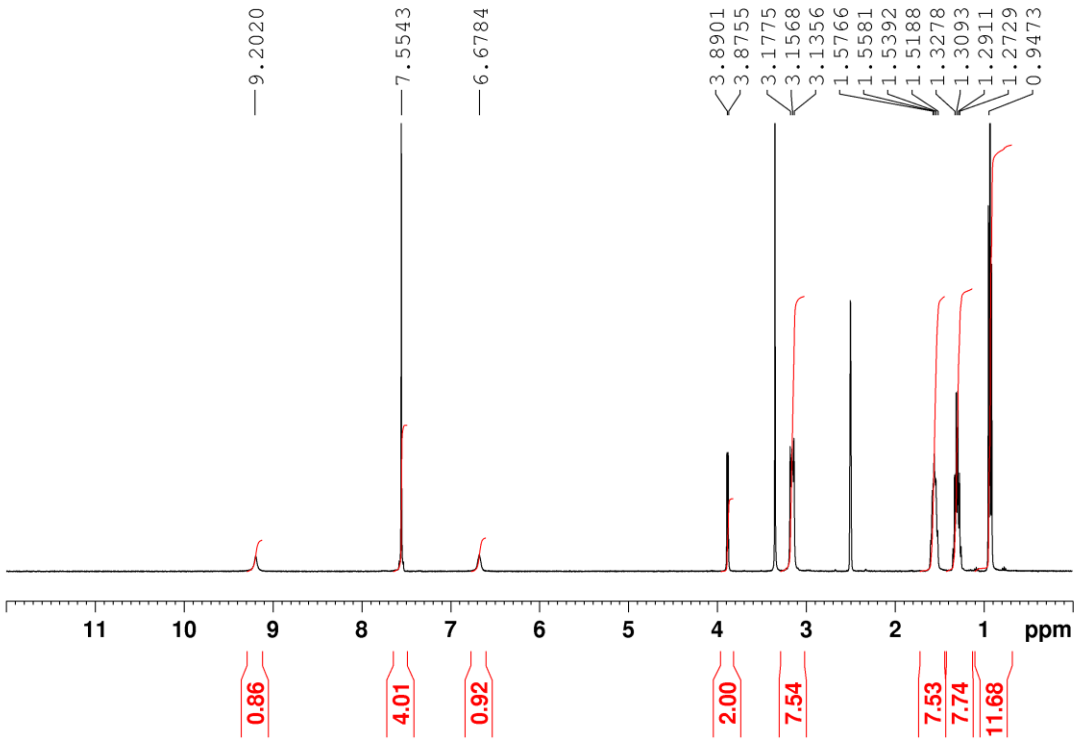

Figure S2. ^{1}H NMR of compound **1** in DMSO-d_6 conducted at 298.15 K.

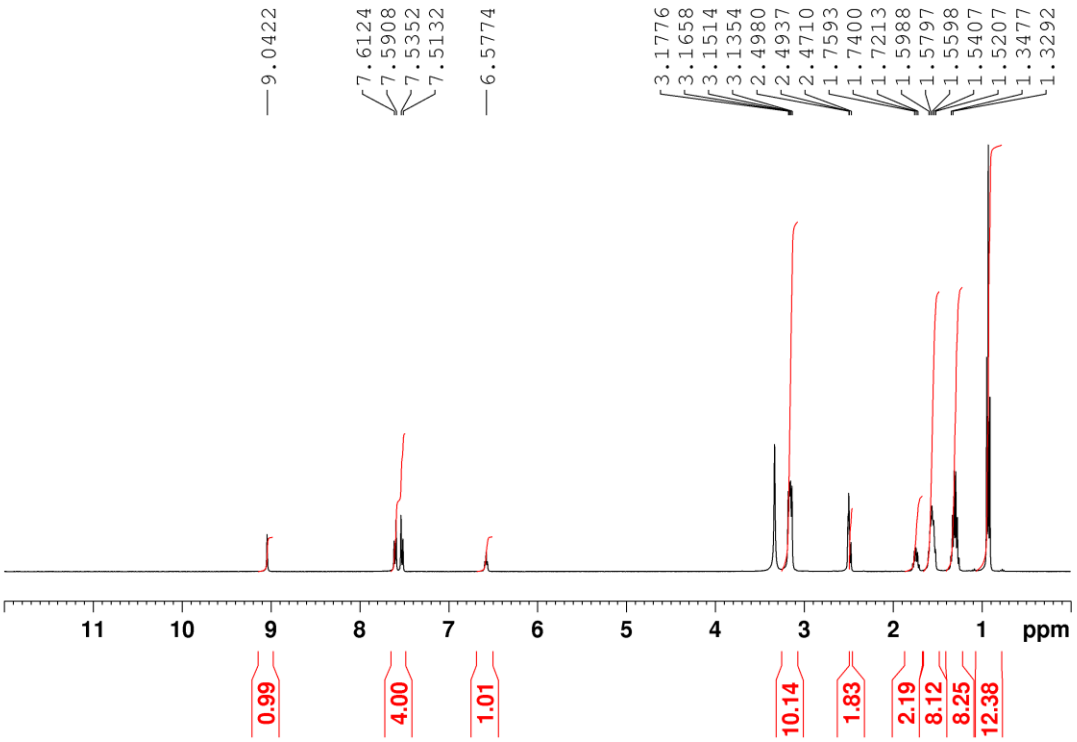

Figure S3. ^{1}H NMR of compound **2** in DMSO-d_6 conducted at 298.15 K.

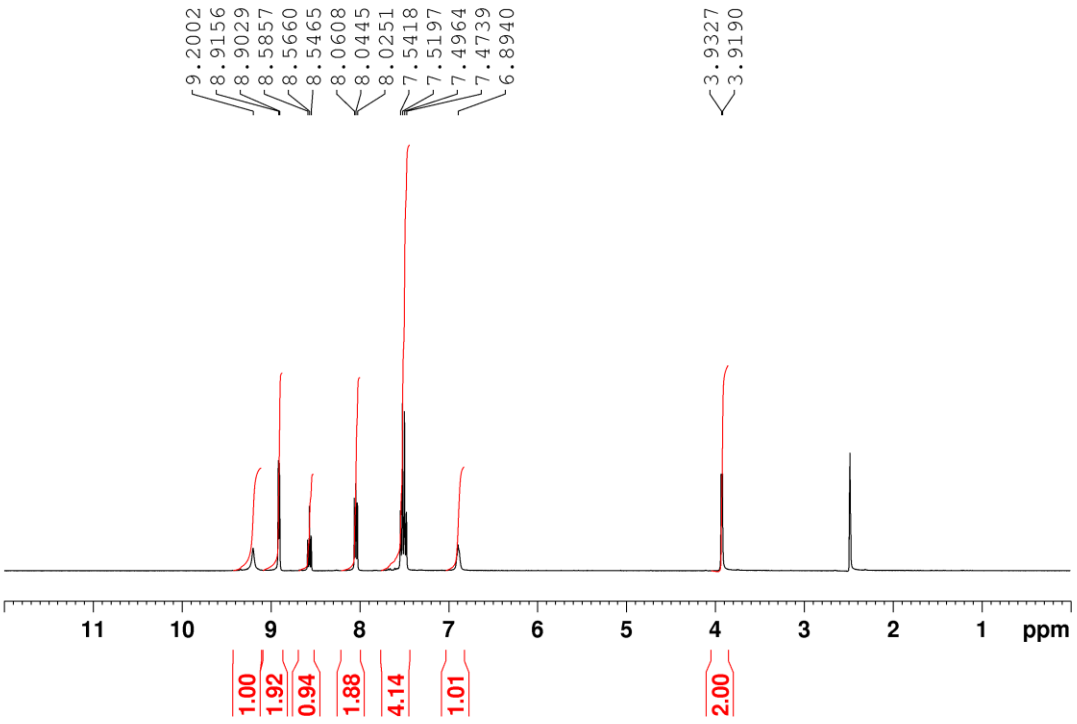

Figure S4. ^{1}H NMR of compound **3** in DMSO-d_6 conducted at 298.15 K.

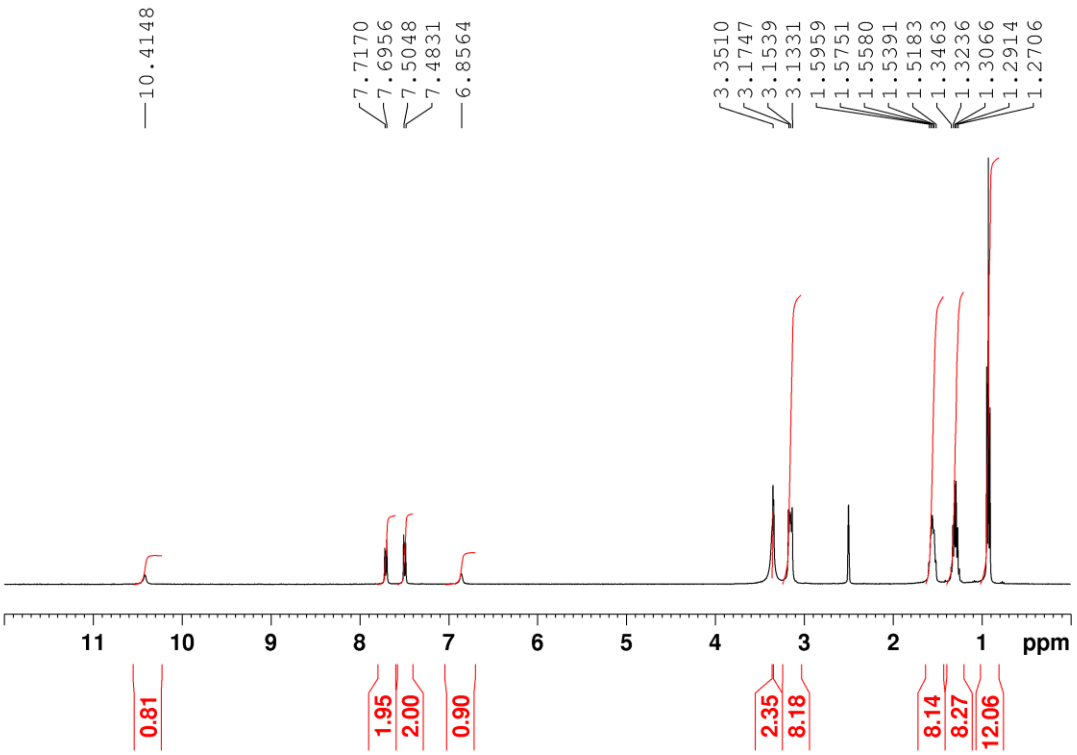

Figure S5. ^{1}H NMR of compound **4** in DMSO-d_6 conducted at 298.15 K.

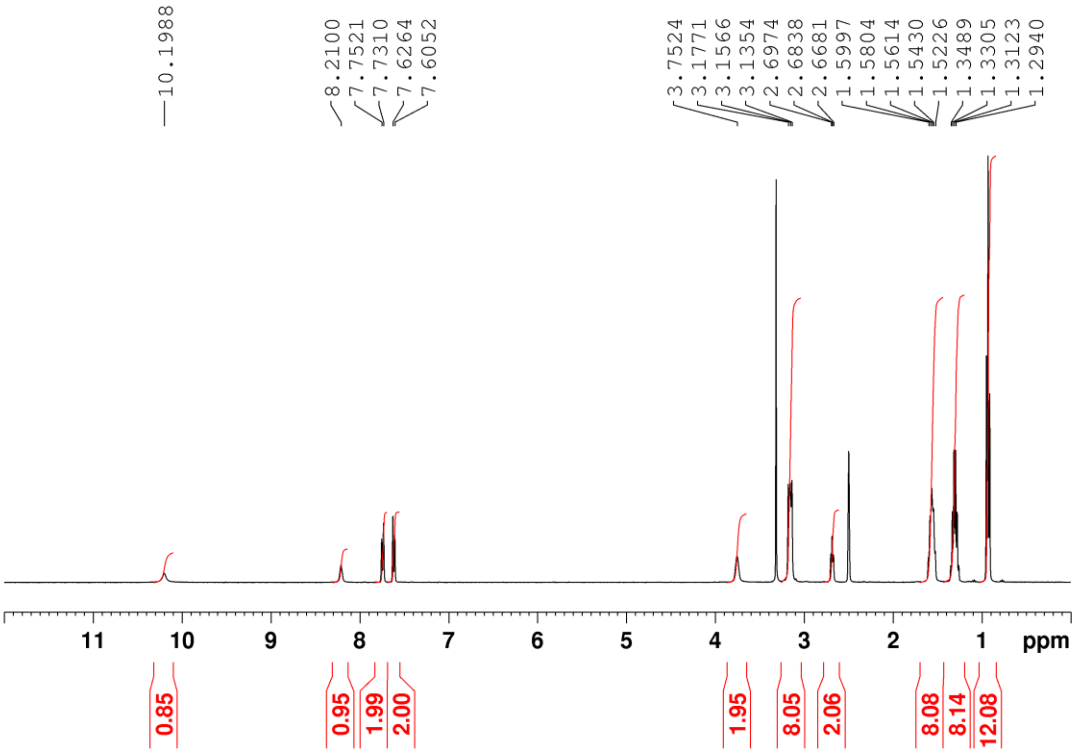

Figure S6. ^{1}H NMR of compound **5** in DMSO-d_6 conducted at 298.15 K.

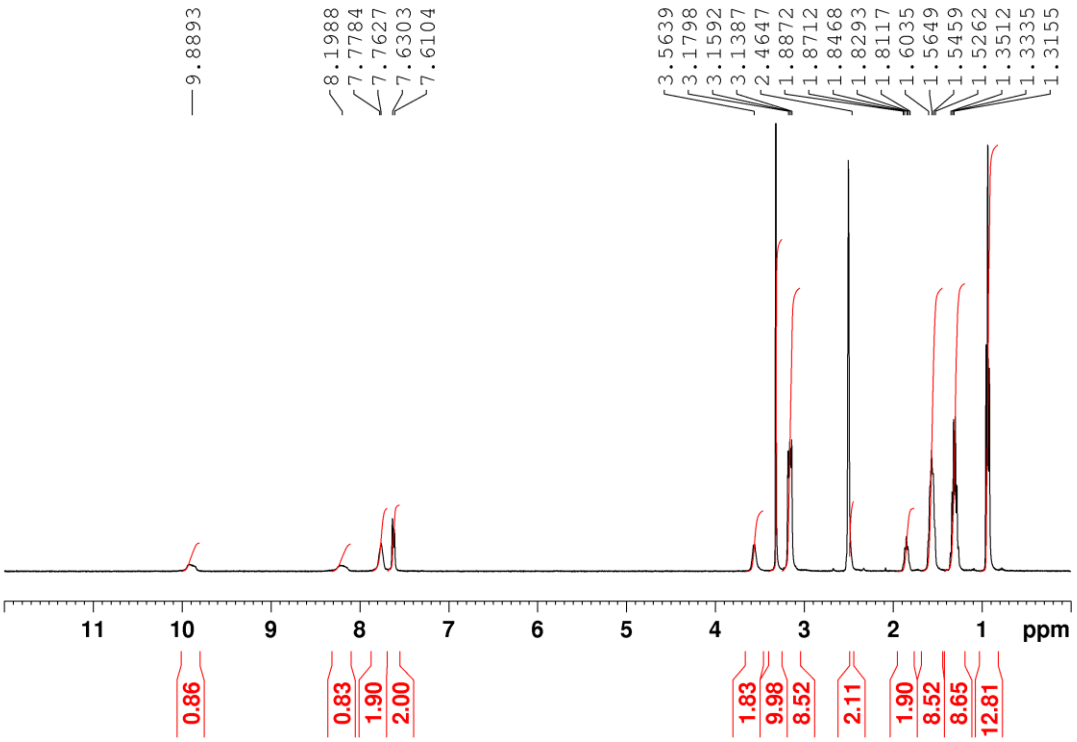

Figure S7. ^{1}H NMR of compound **6** in DMSO-d_6 conducted at 333.15 K.

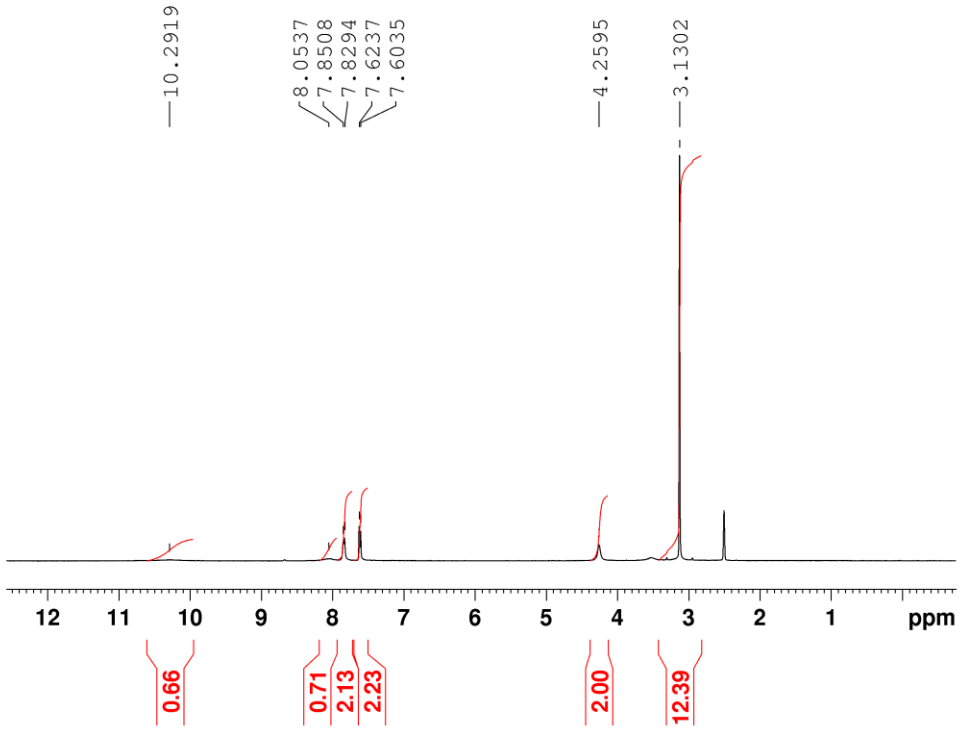

Figure S8. ^{1}H NMR of compound **7** in DMSO-d_6 conducted at 333.15 K.

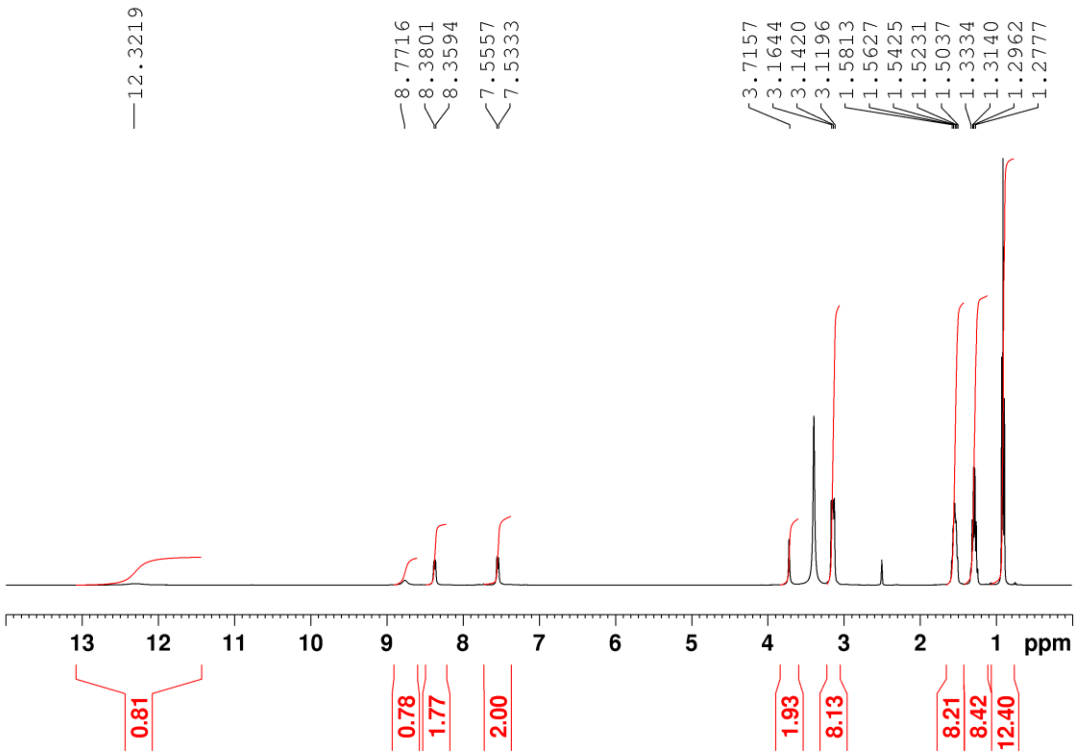

Figure S9. ^{1}H NMR of compound **8** in DMSO-d_6 conducted at 298.15 K.

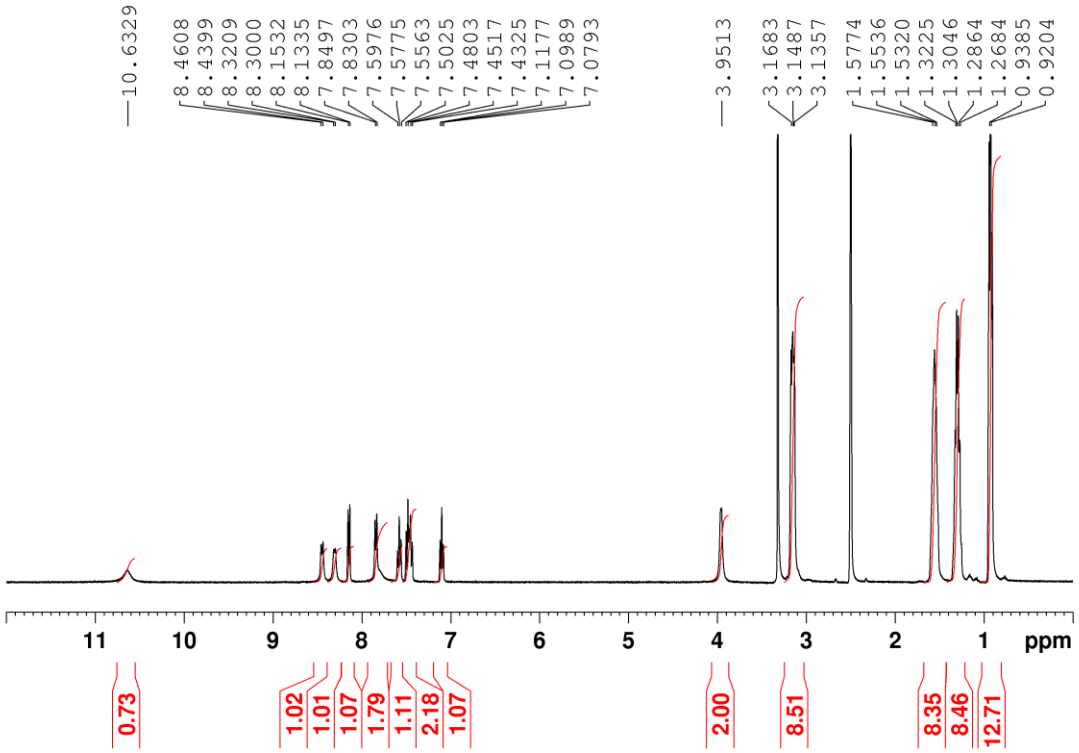

Figure S10. ^{1}H NMR of compound **9** in DMSO-d_6 conducted at 298.15 K.

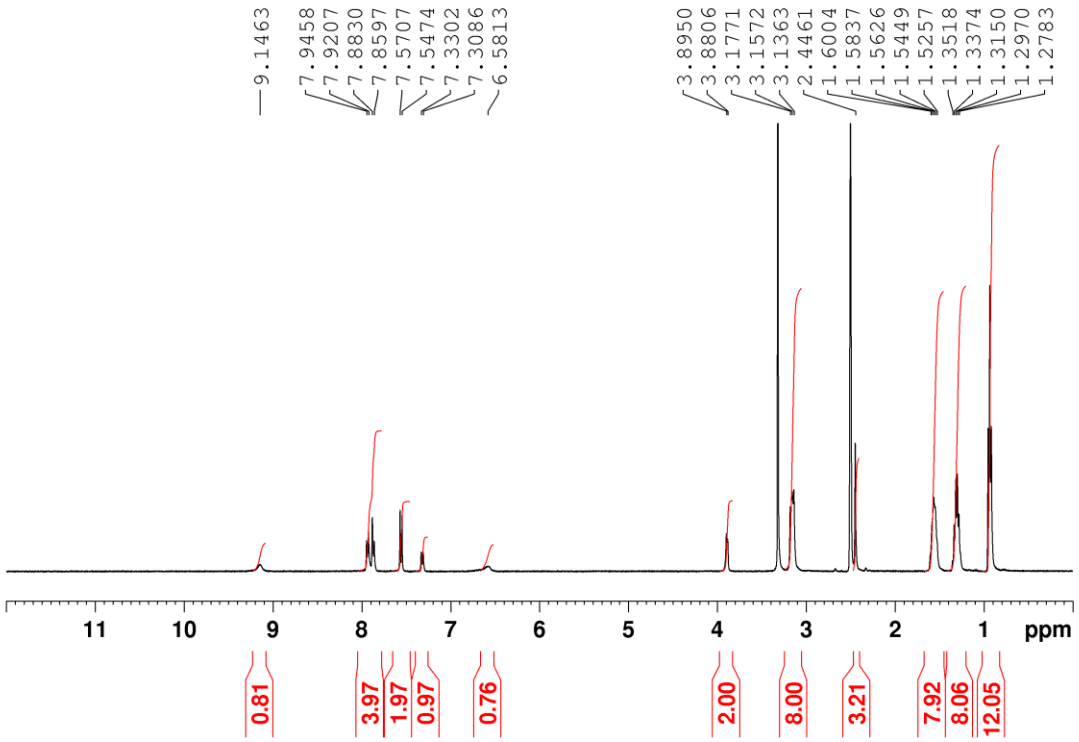

Figure S11. ^{1}H NMR of compound **10** in DMSO-d_6 conducted at 298 K.

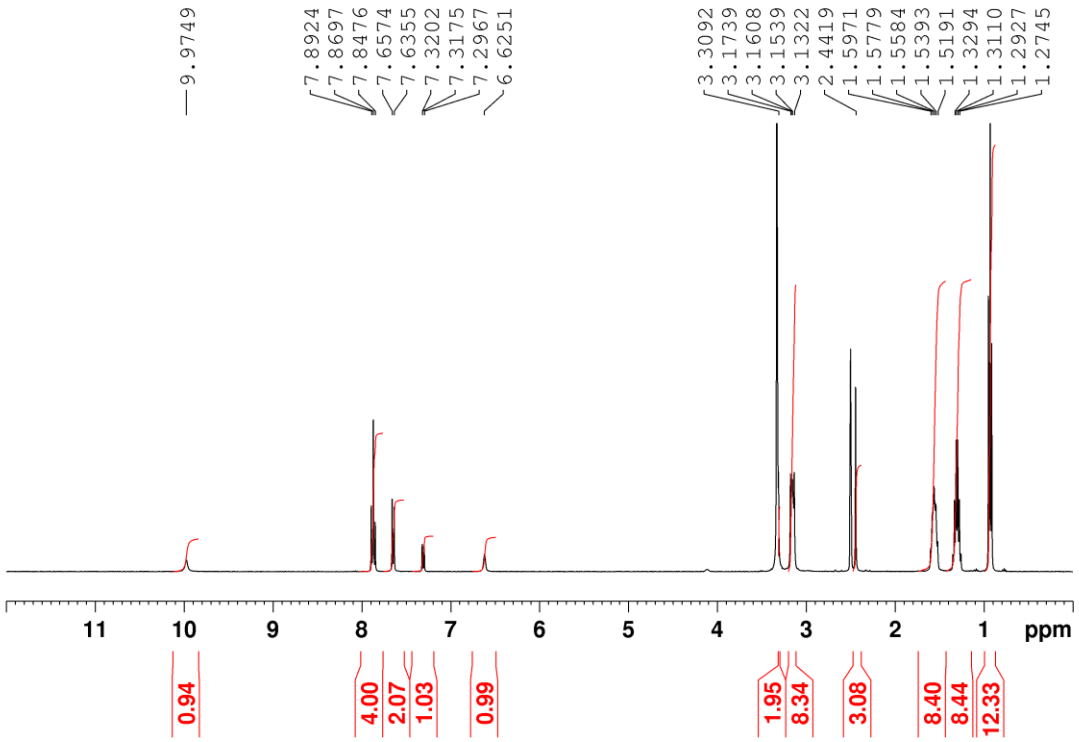

Figure S12. ^{1}H NMR of compound **11** in DMSO-d_6 conducted at 298 K.

Additional Control Data

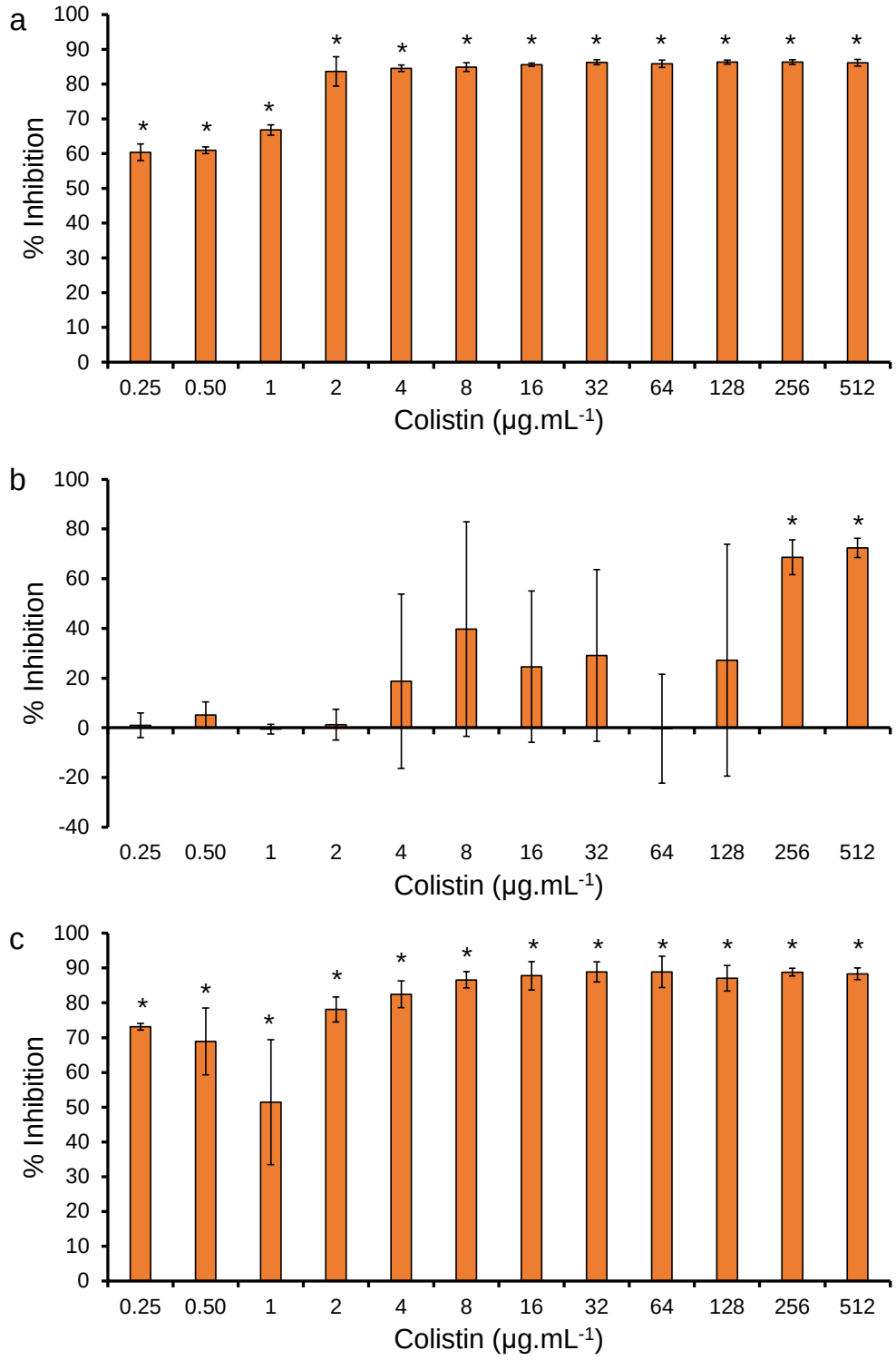

Figure S13. % Inhibition as determined with XTT assay of colistin against a) *P. aeruginosa*, b) *C. albicans*, c) polymicrobial biofilm formation. Cell-free solvent controls and negative controls were included and the percentage inhibition, relative to the negative control, was calculated. Values are the average of all biological and technical repeats and errors bars indicate the standard deviation.

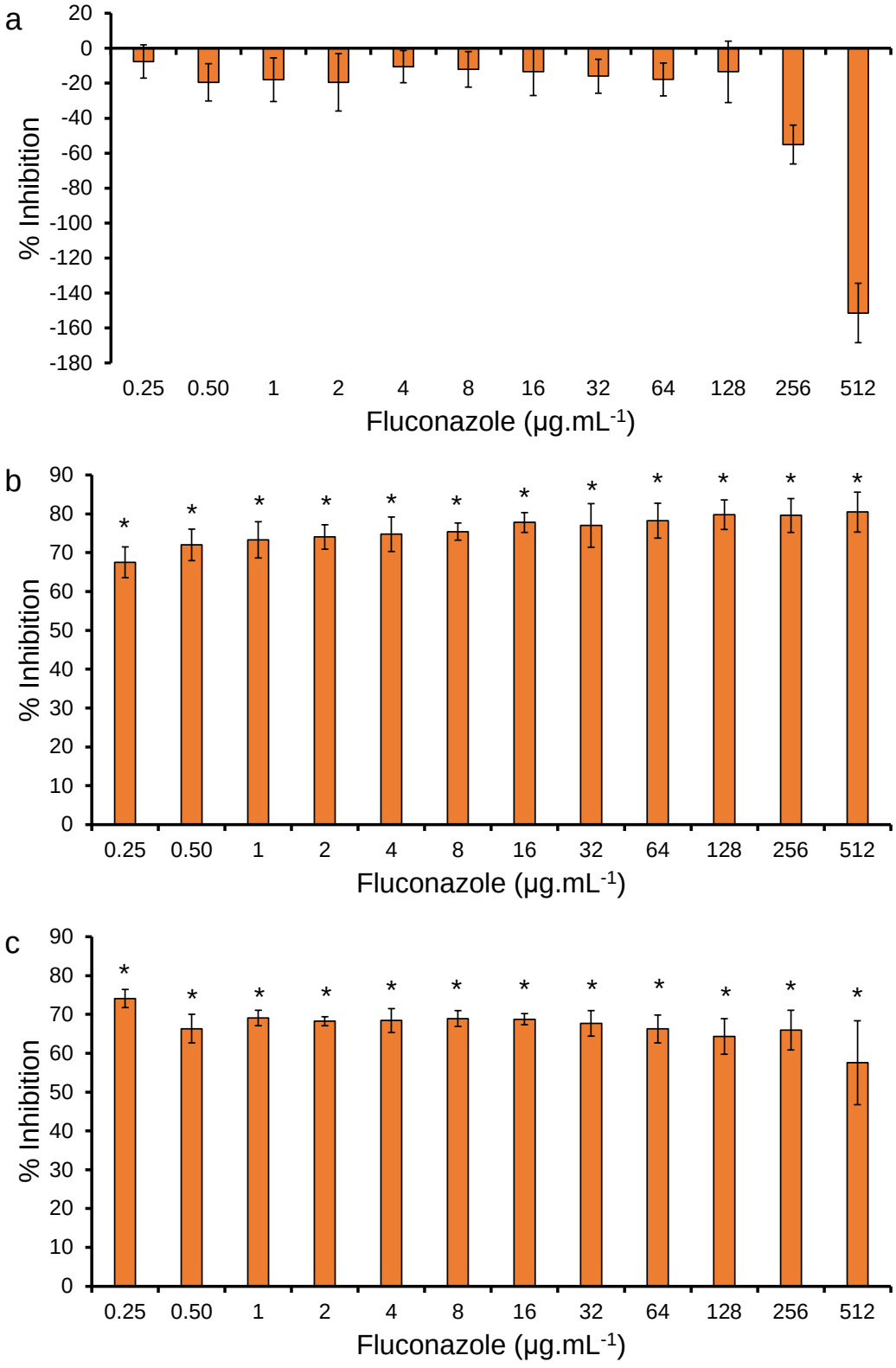

Figure S14. % Inhibition as determined with XTT assay of fluconazole against a) *P. aeruginosa*, b) *C. albicans*, c) polymicrobial biofilm formation. Cell-free solvent controls and negative controls were included and the percentage inhibition, relative to the negative control, was calculated. Values are the average of all biological and technical repeats and errors bars indicate the standard deviation.

References

(1) Hiscock, J. R.; Bustone, G. P.; Wilson, B.; Belsey, K. E.; Blackholly, L. R. *In Situ* Modification of Nanostructure Configuration through the Manipulation of Hydrogen Bonded Amphiphile Self-Association. *Soft Matter* **2016**, *12* (18), 4221–4228. https://doi.org/10.1039/c6sm00529b.

(2) White, L. J.; Tyuleva, S. N.; Wilson, B.; Shepherd, H. J.; Ng, K. K. L.; Holder, S. J.; Clark, E. R.; Hiscock, J. R. Towards the Prediction of Global Solution State Properties for Hydrogen Bonded, Self-Associating Amphiphiles. *Chem. Eur. J.* **2018**, *24* (30), 7761–7773. https://doi.org/10.1002/chem.201801280.

(3) Blackholly, L. R.; Shepherd, H. J.; Hiscock, J. R. 'Frustrated' Hydrogen Bond Mediated Amphiphile Self-Assembly – a Solid State Study. *CrystEngComm* **2016**, *18* (37), 7021–7028. https://doi.org/10.1039/C6CE01493C.

(4) White, L. J.; Tyuleva, S. N.; Wilson, B.; Shepherd, H. J.; Ng, K. K. L.; Holder, S. J.; Clark, E. R.; Hiscock, J. R. Towards the Prediction of Global Solution State Properties for Hydrogen Bonded, Self-Associating Amphiphiles. *Chem. Eur. J.* **2018**, *24* (30), 7761–7773. https://doi.org/10.1002/chem.201801280.

(5) White, L. J.; Wells, N. J.; Blackholly, L. R.; Shepherd, H. J.; Wilson, B.; Bustone, G. P.; Runacres, T. J.; Hiscock, J. R. Towards Quantifying the Role of Hydrogen Bonding within Amphiphile Self-Association and Resultant Aggregate Formation. *Chem. Sci.* **2017**, *8* (11), 7620–7630. https://doi.org/10.1039/c7sc03888g.

(6) Boles, J. E.; Bennett, C.; Baker, J.; Hilton, K. L. F.; Kotak, H. A.; Clark, E. R.; Long, Y.; White, L. J.; Lai, H. Y.; Hind, C. K.; Sutton, J. M.; Garrett, M. D.; Cheasty, A.; Ortega-Roldan, J. L.; Charles, M.; Haynes, C. J. E.; Hiscock, J. R. Establishing the Selective Phospholipid Membrane Coordination, Permeation and Lysis Properties for a Series of 'Druggable' Supramolecular Self-Associating Antimicrobial Amphiphiles. *Chem. Sci.* **2022**, *13*, 9761–9773. https://doi.org/10.1039/d2sc02630a.

(7) Fourie, R.; Ells, R.; Kemp, G.; Sebolai, O. M.; Albertyn, J.; Pohl, C. H. *Pseudomonas aeruginosa* Produces Aspirin Insensitive Eicosanoids and Contributes to the Eicosanoid Profile of Polymicrobial Biofilms with *Candida albicans*. *Prostaglandins Leukot. Essent. Fatty Acids* **2017**, *117*, 36–46. https://doi.org/10.1016/j.plefa.2017.01.008.

(8) Stepanović, S.; Vuković, D.; Dakić, I.; Savić, B.; Švabić-Vlahović, M. A Modified Microtiter-Plate Test for Quantification of Staphylococcal Biofilm Formation. *J. Microbiol. Methods* **2000**, *40* (2), 175–179. https://doi.org/10.1016/S0167-7012(00)00122-6.

(9) O'Toole, G. A. Microtiter Dish Biofilm Formation Assay. *J. Vis. Exp.* **2011**, *47*. https://doi.org/10.3791/2437.